engineering proceedings

Proceeding Paper

Tensile Properties of the Subsurface and Center Regions of AA6111 Direct-Chill-Cast Ingot in Semisolid State and Their Hot Tearing Susceptibility †

Mohamed Qassem [1,*], Mousa Javidani [1], Daniel Larouche [2] and X.-Grant Chen [1]

[1] Department of Applied Science, University of Quebec in Chicoutimi, Saguenay, QC G7H 2B1, Canada; mjavidan@uqac.ca (M.J.); xgchen@uqac.ca (X.-G.C.)
[2] Department of Mining, Metallurgy and Materials Engineering, Laval University, Québec, QC G1V 0A6, Canada; daniel.larouche@gmn.ulaval.ca
* Correspondence: mqassem@etu.uqac.ca
† Presented at the 15th International Aluminium Conference, Québec, QC, Canada, 11–13 October 2023.

Abstract: AA6111 alloys are widely used in the automotive industry owing to their high strength/weight ratio, good corrosion resistance, and reasonable formability. During their manufacture through ingot metallurgy via direct chill (DC) casting, the alloys often suffer from hot tearing, limiting DC casting productivity. The present study focused on evaluating the mechanical properties in the semisolid state and the hot tearing susceptibility of AA6111 DC-cast ingot in the subsurface and center regions. The mechanical behavior of two different regions at high temperatures above solidus was studied using smoothed and notched samples. Tensile tests were performed using the Gleeble 3800 thermomechanical testing unit, and the digital image correlation method was applied to measure the strain evolution. The change in the grain structure in the subsurface and the presence of a high-volume fraction of needle-like β-Fe intermetallics significantly reduced the ductility of the cast ingot in the subsurface region. The hot tearing susceptibility in the subsurface region of the cast ingot was higher than that in the center region. The notch effect is more significant in the subsurface on the stress sensitivity in the presence of stress raisers compared with that in the center region.

Keywords: AA6111 DC-cast alloy; high-temperature tensile properties; hot tearing susceptibility; brittle temperature range

Citation: Qassem, M.; Javidani, M.; Larouche, D.; Chen, X.-G. Tensile Properties of the Subsurface and Center Regions of AA6111 Direct-Chill-Cast Ingot in Semisolid State and Their Hot Tearing Susceptibility. *Eng. Proc.* **2023**, *43*, 9. https://doi.org/10.3390/engproc2023043009

Academic Editor: Mario Fafard

Published: 12 September 2023

1. Introduction

Among the Al-Mg-Si 6xxx series, AA6111 alloy is preferred in body panels because of its high strength-to-weight ratio, reasonable deformability, and good surface finish [1]. The main challenge in increasing the productivity of AA6111 DC-cast ingots is to avoid the formation of hot tears during casting [2]. Hot tearing is a critical defect developed during solidification because of two main reasons: inadequate liquid feeding and excessive thermal stresses [3]. Therefore, measuring the mechanical properties of alloys in a semisolid state is beneficial to set the limits of stress and strain over which hot tears may develop during casting. Tensile testing upon reheating is one commonly used method to characterize semisolid mechanical properties because of its ability to obtain quantitative results [4]. However, measuring the strain of semisolid samples is a challenging task because traditional methods, e.g., extensometers, exert significant stress by their direct contact. Recently, the digital image correlation (DIC) method was shown to solve this problem as it is contactless and has high accuracy [5].

During the DC casting process, the subsurface region of the ingot is initially under tensile stresses, while the ingot center is under compressive stresses. Once the ingot starts cooling down, the state of stresses changes inversely in both zones [6]. The surface zone differs from the center zone in several aspects, e.g., macro-segregation, localized cooling rate, grain size, and type of intermetallic phases [7,8]. Several studies observed coarsening of dendritic arm spacing and grain size with moving toward the center of the ingot [9–11]. In DC casting, the local cooling rate varies from 1 K/s in the ingot center to 20 K/s near the ingot surface [12].

Intermetallic morphology and its distribution have a great impact on hot tearing susceptibility. One of the main intermetallic phases responsible for crack initiation during casting is Fe-rich intermetallic. It was reported that β-Fe intermetallic with its needle-like shape can initiate cracks and prevent liquid feeding during solidification [12,13]. Mn addition to the 6xxx series was found to increase the preference for the formation of α-Fe instead of β-Fe. The formation of needle-like shaped β-Fe is not only dependent on chemical composition but also highly localized cooling. On the other hand, low melting eutectic phases, e.g., Cu-rich phases, were reported to play an important role in the formation of liquid films at high solid fractions above solidus temperature [2,14].

Stress triaxiality controls the macroscopic strain that occurs during DC casting [15]. The mechanical behavior of semisolid AA6111 under stress triaxiality conditions has rarely been reported in the literature. The present study focused on evaluating the semisolid tensile properties and the hot tearing susceptibility of AA6111 DC-cast ingots in the subsurface and center regions. The tests were performed using the smoothed samples at a temperature range of 510–580 °C to determine the brittle temperature range [2]. The notched samples at two temperatures (530 and 550 °C) were then tested to characterize the notch effect. The as-cast microstructure of the ingot was examined using optical microscopy, and fracture surfaces after the tensile test were analyzed using a scanning electron microscope. Based on microstructural and mechanical results, the hot tearing susceptibility in both regions was evaluated.

2. Experimental Procedure

The cast ingot examined in this study is a commercial wrought AA6111 alloy, and its actual chemical composition is listed in Table 1. The 6111 alloy with such chemistry had high hot tearing susceptibility [2], and the cast ingot had a large crack propagated along the rolling surface after casting. The DC-cast ingot was provided by the Arvida Research and Development Centre of Rio Tinto Aluminum. The grain structure was characterized under polarized light in the optical microscope (Nikon ECLIPSE ME 600, Nikon Co, Tokyo, Japan) after electro-etching using Barker's reagent (3 vol% HBF4 solution) at 40 V for 3 min. The quantitative analysis of secondary intermetallic phases in the subsurface and center regions was evaluated based on a minimum of 50 images at a magnification of 200× using image analysis. The fracture surface of fractured tensile samples was cleaned using ultrasonic waves, and then analyzed using a scanning electron microscope (SEM, JSM-6480 LV, JEOL Ltd., Tokyo, Japan).

Table 1. Chemical composition of the cast ingot studied (wt.%).

Mg	Mn	Fe	Cu	Si	Ti	Al
0.6	0.2	0.2	0.7	0.7	0.03	Bal.

Tensile samples were sectioned from two different locations of the ingot parallel to the casting direction. The first location was the subsurface region (3 mm from the cast surface) and the second one was in the center of the ingot. The cross-section of the ingot slice was 590 mm in length and 185 mm in width. Two types of samples were used in this study: smoothed and double-V notched, as shown in Figure 1. Tensile tests of the smoothed samples were performed using the Gleeble 3800 at four temperatures: 510, 530, 550, and 580 °C, using a displacement rate of 0.1 mm/s. For the notched samples, the tests were performed at 530 and 550 °C. Tensile samples were heated to the testing temperature at a heating rate of 2 °C/s, soaked for 1 min, and then the test was conducted. For each condition, 2–3 samples were tested depending on the repeatability of the results.

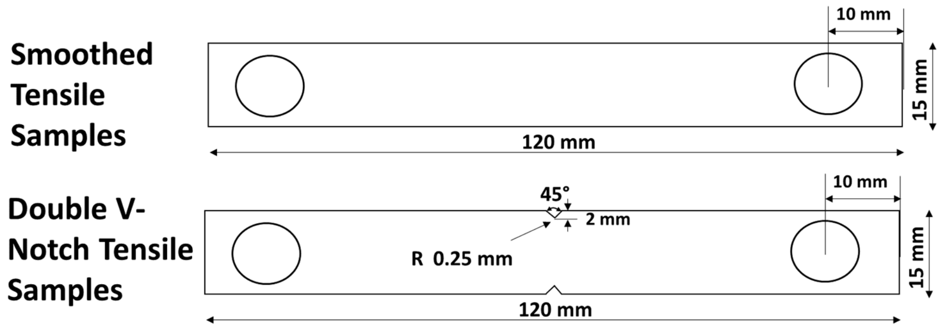

Figure 1. Dimensions of tensile samples for the smoothed and double-V notched types.

The strain was measured by DIC. The DIC method is an optical technique, which utilizes the full-field, non-contact, and high-precision measurement of deformation and displacement. A ceramic spray was used to obtain the speckle pattern on the sample's surface, as shown in Figure 2. The initial gauge length was 2 mm, where the distance between the centroids of the subsets is the gauge length (Figure 2a). The distance between both centroids was followed during the tensile test until fracture (Figure 2b). It was reported that the resolution of the DIC method is 0.09 µm [2]. Images were captured at a rate of 20 frames per second. All the captured images were converted to a grayscale pattern, 800 × 450 in size. Then, these images were analyzed using the GOM Correlate software (Germany), which measured the displacement based on the change in length of the 2 mm reference line during the test.

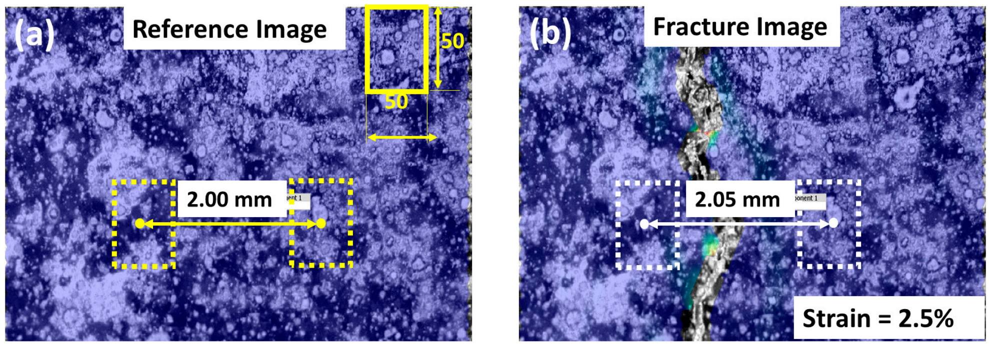

Figure 2. Schematic showing how GOM correlate software measures the displacement relative to the reference image (initial gauge length of 2 mm), where the initial subsets are yellow and deformed subsets are white.

3. Results

3.1. As-Cast Microstructure

The as-cast microstructures of both regions (subsurface and center) are presented in Figure 3a,b, which consisted of α-Al dendrite cells/grains and several intermetallic phases distributed in the interdendritic regions, including Mg_2Si, two Fe-rich intermetallics (α-$Al_{15}(Fe,Mn)_3Si_2$ and β-$Al_5(Fe,Mn)Si$), and two Cu-bearing intermetallics (Q-$Al_5Mg_8Si_6Cu_2$ and θ-Al_2Cu). The intermetallic phases were identified based on their morphologies and SEM-EDS analysis results. The primary Mg_2Si phase appeared in dark lamellar form, whereas the bright areas are attributed to Cu-bearing phases. Fe-rich intermetallics appeared in three forms: needle, platelet, and blocky forms. The color of Fe-rich intermetallics was gray. The volume fractions of all phases are presented in Figure 4. It was reported that the high rate of thermal contraction and solidification shrinkage at the surface region compared to the center region of the ingots could drive the deformation-induced liquid flow toward the surface region, producing large segregation [7]. Consequently, DC-cast ingots may exhibit different fractions of intermetallic phases at surface and center regions.

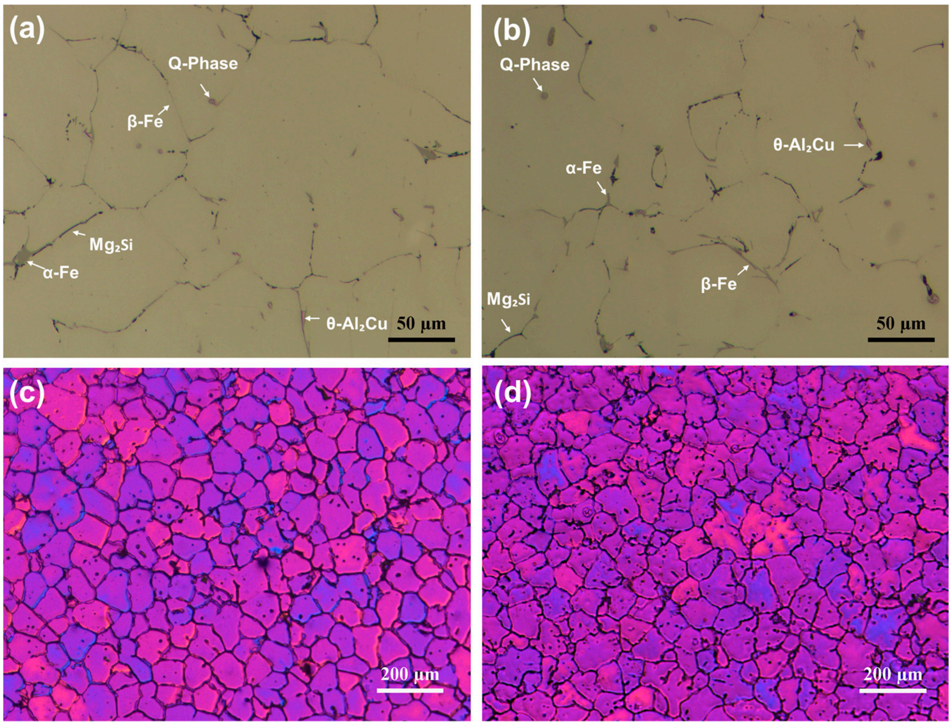

Figure 3. As-cast microstructure and grain structure in both regions: (**a**,**c**) the subsurface and (**b**,**d**) the center.

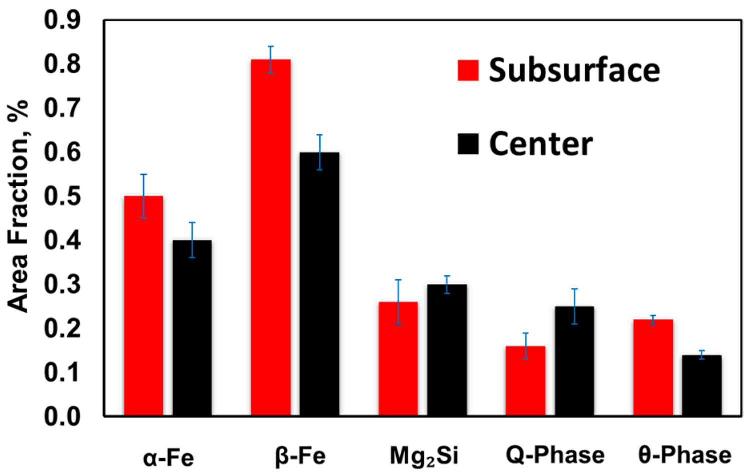

Figure 4. Volume fraction of different intermetallic phases in both locations of the ingot.

Two different Cu-rich phases were detected in the microstructure, where Al_2Cu appeared as small blocks and Q-phase appeared as spheroids. The most dominant Cu-rich phase in the subsurface region was Al_2Cu, while the Q-phase was more prevalent in the center region. The volume fraction of Al_2Cu decreased from 0.22 vol.% at the subsurface to 0.14% at the center, whereas the volume fraction of the Q-phase increased from 0.16% to 0.25% moving from the subsurface to the center.

The morphology and (Fe+Mn)/Si ratio were used to identify two Fe-rich intermetallic phases. The α-$Al_{15}(Fe,Mn)_3Si_2$ exhibited Chinese-script morphology with a (Fe+Mn)/Si ratio of ~1.5. In contrast, the β-$Al_5(Fe,Mn)Si$ exhibited a needle-like shape with a (Fe+Mn)/Si ratio of ~0.8. These methods of identifying Fe-intermetallic were proved to be effective in identifying Fe-intermetallics in the literature [2]. The aspect ratio (length/width) of β-Fe was larger than that of α-Fe. The volume fraction of β-Fe was 0.81% in the subsurface and

0.62% in the center region. In addition, the aspect ratio of β-Fe in the subsurface was higher than that in the center region (32.4 ± 5.2 vs. 17.3 ± 4.2).

Both regions showed different grain structures, where the equiaxed cellular structure appeared in the subsurface region and the equiaxed dendritic structure occurred in the center region. The average grain sizes in both regions are nearly similar (~75 μm). With the equiaxed cellular morphology, the permeability within the dendrite envelope is zero, and fluid flow will only take place in the dendritic region [16], resulting in the easy formation of cracks because of the poor permeability and interlocking. In addition, the β-Fe appeared as needle-like shaped in the subsurface (Figure 3a). It was reported that needle-like shaped β-Fe were preferentially formed at a high cooling rate, e.g., in the surface region of DC-cast ingots [17]. As the cooling rate reduced, most of β-Fe appeared as blocky and platelet particles, as shown in Figure 3b. It was also reported that needle-like particles were likely to act as crack initiators because of the stress concentration in the sharp tips [13].

3.2. Mechanical Behavior in the Semisolid State

The evolution of the tensile strength and fracture strain of smoothed samples with increasing temperature is presented in Figure 5. The solidus temperature of the alloy is 510 °C, and the temperature range for the tensile tests was selected from 510 to 580 °C, representing the fraction of solid (f_s) from 1 to 0.92 [2], which covers the most sensitive solid fraction range for hot tearing. As shown in Figure 5a, the tensile strength decreased with increasing temperature in both subsurface and center regions, and the strength values of both regions were close to each other in the semisolid range studied. The strength decreased from 22.5 MPa at 510 °C to 4–7 MPa at 580 °C. Toward the maximum temperature of 580 °C, the strength is slightly higher in the center region than in the subsurface region.

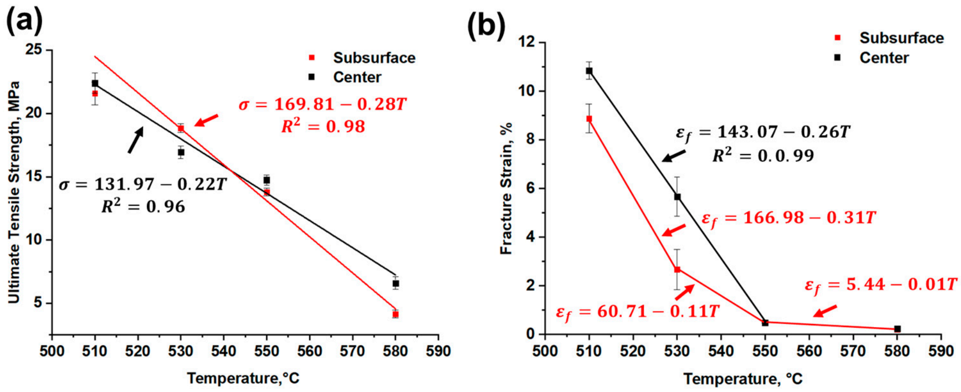

Figure 5. Tensile properties as a function of the temperature in the semisolid state: (**a**) tensile strength and (**b**) fracture strain.

On the other hand, the fracture strain also decreased with increasing temperature, and the variation in fracture strain with temperature can be divided into two stages in the center region and three stages in the subsurface region, as shown in Figure 5b. Up to 550 °C, the fracture strains in the subsurface region are always lower than in the center region. From 550 to 580 °C, the fracture strain in both regions was almost close to zero. It was reported that the material exhibited a zero-ductility condition when its fracture strain reached 3% [2,18]. The fracture strain in the subsurface reached the zero-ductility condition at 530 °C, while the same strain was obtained in the center at 540 °C. The subsurface reached the zero-ductility condition more rapidly than in the center, which is likely attributed to the partial melting of its higher volume fraction of Al_2Cu (0.22%) compared with the center region (0.14%) (Figure 4).

3.3. Mechanical Behavior of Notched Samples

The notched sample tests were used to study the mechanical behavior under triaxiality conditions [19]. Stress triaxiality may develop during the DC casting process because of the presence of stress raisers, e.g., inclusions, oxide films, and brittle intermetallics. The notch strength ratio (NSR, the ratio of UTS of the notched sample to UTS of the unnotched sample) can be used to describe the behavior of the material in the presence of triaxial stresses: the notch strengthening in ductile materials (NSR > 1) or notch weakening in brittle materials (NSR < 1) [19]. The stress–strain curves of notched samples in two temperatures are presented in Figure 6a. At the low temperature of 530 °C, the stress was higher in the subsurface than in the center. In contrast, the stress in the center was higher than in the surface at 550 °C. At both temperatures, the strains in the subsurface were always lower than those in the center. The increase in temperature from 530 to 550 °C resulted in a large reduction in both strength and strain. From the stress–strain curve, the strain energy per unit area required for fracture can be derived from the area under the curve, which is named the modulus of toughness [20]. At 550 °C, the modulus of toughness of the subsurface is calculated to be 0.023 MJ/m^3, which is lower than that of the center region (0.041 MJ/m^3). This indicates that the resistance of the subsurface to fracture is lower than that of the center at 550 °C.

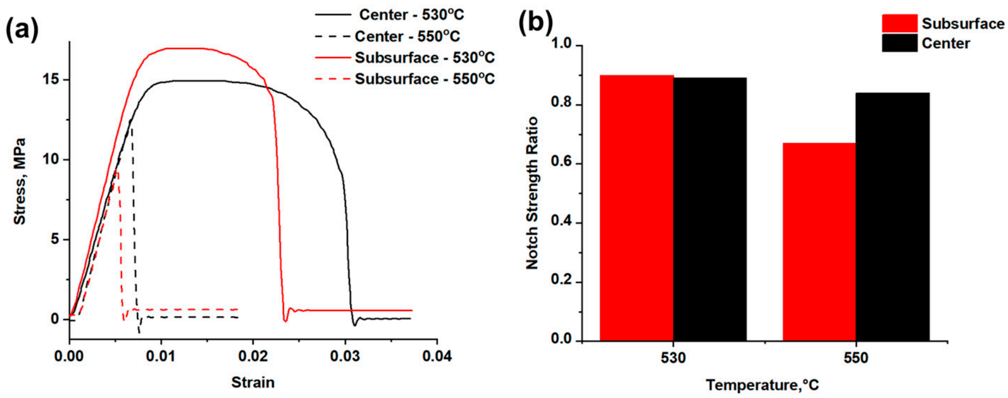

Figure 6. Tensile properties of notched samples tested at 530 and 550 °C: (**a**) stress–strain curves and (**b**) notch strength ratio (NSR).

As shown in Figure 6b, the NSR at 530 °C in both regions is similar, while it is different at 550 °C. The subsurface showed the highest reduction in its strength from 15 MPa in the smoothed samples to 9 MPa in the notched samples at 550 °C, so its NSR of 0.67 was lower than that in the center (NSR = 0.82). It was reported that the notch weakening happens if the NSR is lower than 1 [19], which is the dominant case in the semisolid state. A reduction in NSR is an indication of a high notch effect and a large reduction in strength in the presence of the notch. The large notch effect in the subsurface at 550 °C indicates that the stress developed by stress raisers during casting may have a severe impact in the subsurface region, where the cracks may easily evolve. As the strength and strain of the subsurface were the worst at 550 °C, it is the preferred site in the cast ingot for forming hot tearing.

3.4. Fracture Surfaces of Notched Samples

Fracture surfaces of notched tensile samples were analyzed to explore the effect of the temperature on the fracture mechanism. The tensile behavior of notched samples in the subsurface at 530 °C showed moderate plastic deformation, but without any plastic deformation at 550 °C (Figure 6a). The fracture surface of tensile samples tested at 530 °C is a mixed fracture mode between intergranular (I-crack) and transgranular (T-crack), as shown in Figure 7a. As the temperature increases to 550 °C, the dominant fracture is the intergranular type, and the smooth grain surface after fracture indicates the brittle nature (Figure 7b).

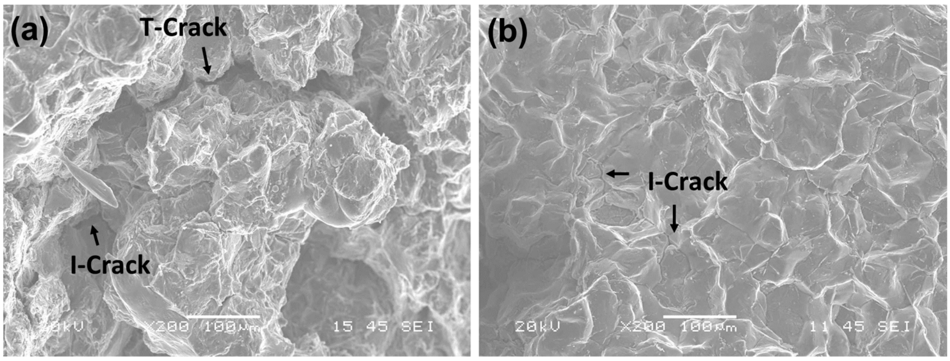

Figure 7. Fracture surfaces of notched tensile samples in the subsurface tested at (**a**) 530 °C and (**b**) 550 °C.

As mentioned in the previous section, notched samples of the center region showed better tensile properties compared with the subsurface region at 550 °C (Figure 6a). In the fracture surface of notched samples of the center region at 550 °C (Figure 8), solid bridges were observed across intergranular cracks. Compared with the fracture surface of notched samples in the subsurface region (Figure 7b), it is believed that those bridges between liquid films surrounding grains provided higher strength and strain in the center region relative to the subsurface region. By analyzing the solid bridges using EDS, it was found that it was mainly eutectic of α-Al+Mg_2Si+Si.

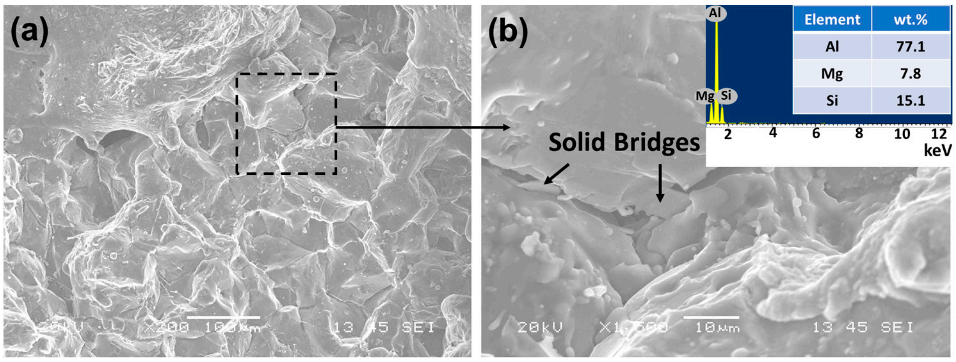

Figure 8. The fracture surface of notched tensile samples in the center region tested at 550 °C.

4. Discussion

As-cast microstructures of the cast ingot showed different grain morphologies in both regions (Figure 3c,d). The subsurface region solidified in equiaxed cellular form, while the center region showed equiaxed dendrite grains. It was reported that the branched network of equiaxed dendritic grains delayed the formation of liquid film by trapping the liquid, and hence increased the crack propagation resistance [18]. On the other hand, poor interlocking in equiaxed cellular grains was found to reduce the resistance to crack propagation [16,19]. Therefore, the fracture strain of the subsurface was considerably lower than that of the center region (Figure 5b). The change in grain structure was not the only reason for the strain reduction—the morphology and quantity of intermetallic phases also played a significant role.

It was reported that one of the main fracture mechanisms at elevated temperatures was decohesion along the interface between Fe-rich intermetallic and the α-Al matrix [20]. When the Fe-rich intermetallics are needle-like, the interfacial energy increases, providing an active pathway for cracks to propagate [21]. In this study, the needle-like β-Fe with a larger aspect ratio of 32 was formed in the subsurface region compared with the lower aspect ratio of 17 in the center region. Moreover, the higher volume fraction of β-Fe in the subsurface provided more crack initiation sites, forming more pathways for crack propagation compared with the center region. On the other hand, the most dominant Cu-rich phase in the subsurface was Al_2Cu, while Q-phase was the most dominant in the center zone. The liquid films of eutectic Al-Al_2Cu at a relatively low temperature (510–550 °C) can attach to the surface of Fe-rich intermetallics, forming pathways for crack progression. As the subsurface region had higher volume fractions of Al_2Cu and needle-like β-Fe (Figure 4), the cracks could more easily propagate in the subsurface compared with the center region, corresponding to a low tensile ductility in the subsurface. This mechanism of crack formation in the semisolid state of Al-Mg-Si alloy was previously reported [14,22].

Based on the tensile properties in the semisolid state (Figure 5), two critical temperatures were determined The lowest boundary temperature was the zero-ductility temperature (ZDT), corresponding to a fracture strain of 3%, and the highest boundary temperature was the zero-strength temperature (ZST), where strength was nearly zero. According to these two temperatures, the brittle temperature range (BTR) was calculated in both regions. The ZDT of the subsurface was 530 °C, while it was 540 °C for the center zone. For the ZST, it was 580 °C in both regions. Therefore, the BTR in the subsurface was 50 °C, which is higher than that in the center region by 10 °C. It was confirmed that a wider BTR promotes higher hot tearing susceptibility in Al alloys [23]. In brief, the hot tearing susceptibility of the subsurface is higher than that of the center zone. In our previous work [2], the BTR of this type of AA6111 alloy was 50 °C, which is similar to the BTR at the subsurface in this study.

Finally, the notch effect was studied to evaluate the stress sensitivity in the presence of stress raisers. The fracture strains of notched samples in the center region were always larger than those of the subsurface. As the subsurface region had a higher volume fraction of needle-like β-Fe intermetallics that act as a stress raiser, the notch effect is more significant in the subsurface. At 550 °C, the strength of the subsurface region was reduced from 15 MPa in the smoothed sample to 9 MPa in the notched sample, resulting in a lower NSR in the subsurface relative to the center region. On the other hand, the strength of the center region was not reduced significantly because of its ability to form solid bridges by eutectic phases (α-Al+Mg_2Si+Si). Consequently, the notch effect had more of an impact in the subsurface region during solidification, and any stress raisers in the ingot subsurface might easily develop as cracks and hot tears during the last stage of solidification.

5. Conclusions

The mechanical behavior of an AA6111 DC-cast ingot in the semisolid state for the subsurface and center regions was investigated. This study used two different types of tensile samples: smoothed and notched samples. The hot tearing susceptibility of both regions was evaluated based on the brittle temperature range of the smoothed samples and the notch effect using the notched samples. The following conclusions can be drawn.

- The tensile strengths in the semi-solid range (covering fs from 1 to 0.92) in the subsurface and center regions were mostly similar. However, the fracture strains in the center region were significantly higher than those in the subsurface region. The low tensile ductility of the subsurface is likely attributed to the poor interlocking of the equiaxed cellular grain structure and the higher volume fraction of needle-like β-Fe intermetallics, which reduced the resistance to crack initiation.
- The hot tearing susceptibility in the subsurface region of the cast ingot was higher than that in the center region. The brittle temperature range of the subsurface was wider than that in the center region.
- The notch effect is more significant in the subsurface on the stress sensitivity in the presence of stress raisers compared with that in the center region, indicating that the occurrence of hot tearing in the subsurface is favored.

Author Contributions: Methodology, M.Q.; software, M.Q.; formal analysis, M.Q.; investigation, M.Q.; writing—original draft preparation, M.Q.; conceptualization, M.J., D.L. and X.-G.C.; validation, M.J., D.L. and X.-G.C.; writing—review and editing, M.J., D.L. and X.-G.C.; funding acquisition, D.L. and X.-G.C.; project administration, X.-G.C. All authors have read and agreed to the published version of the manuscript.

Funding: This research was funded by the Natural Sciences and Engineering Research Council of Canada (NSERC) under Grant No. CRDPJ 514651-17, Fonds de recherche du Québec-Nature et technologies (FRQNT) under Grant No. 2018-LU-252831, and the Mitacs Acceleration under Grant No. IT14722.

Institutional Review Board Statement: Not applicable.

Informed Consent Statement: Not applicable.

Data Availability Statement: The data are available on request.

Acknowledgments: The authors would like to acknowledge the support of the Natural Sciences and Engineering Research Council of Canada, Rio Tinto Aluminum, Fonds de recherche du Québec-Nature et technologies, and Mitacs in this project. Special thanks are given to Josée Colbert of Rio Tinto Aluminum for initiating the project and preparing the cast ingots.

Conflicts of Interest: The authors declare no conflict of interest.

References

1. Engler, O.; Hirsch, J. Texture control by thermomechanical processing of AA6xxx Al–Mg–Si sheet alloys for automotive applications—A review. *Mater. Sci. Eng. A* **2002**, *336*, 249–262. [CrossRef]
2. Qassem, M.; Javidani, M.; Larouche, D.; Colbert, J.; Chen, X.-G. Effect of chemical composition on the semisolid tensile properties and hot tearing susceptibility of AA6111 DC cast alloys. *J. Mater. Sci.* **2022**, *57*, 21519–21536. [CrossRef]
3. Li, Y.; Li, H.; Katgerman, L.; Du, Q.; Zhang, J.; Zhuang, L. Recent advances in hot tearing during casting of aluminium alloys. *Prog. Mater. Sci.* **2020**, *117*, 100741. [CrossRef]
4. Eskin, D.; Suyitno; Katgerman, L. Mechanical properties in the semi-solid state and hot tearing of aluminium alloys. *Prog. Mater. Sci.* **2004**, *49*, 629–711. [CrossRef]
5. Mitchell, J.; Cockcroft, S.; Viano, D.; Davidson, C.; StJohn, D. Determination of strain during hot tearing by image correlation. *Metall. Mater. Trans. A* **2007**, *38*, 2503–2512. [CrossRef]
6. Alhassan-Abu, A.; Wells, M. Determination of constitutive behaviour of as cast AA 5182 for deformations that occur during direct chill casting using the Gleebe 1500 machine. *Mater. Sci. Technol.* **2003**, *19*, 55–61.
7. Nadella, R.; Eskin, D.; Du, Q.; Katgerman, L. Macrosegregation in direct-chill casting of aluminium alloys. *Prog. Mater. Sci.* **2008**, *53*, 421–480. [CrossRef]
8. Sengupta, J.; Thomas, B.G.; Wells, M.A. The use of water cooling during the continuous casting of steel and aluminum alloys. *Metall. Mater. Trans. A* **2005**, *36*, 187–204. [CrossRef]
9. Suyitno; Eskin, D.; Katgerman, L. Structure observations related to hot tearing of Al–Cu billets produced by direct-chill casting. *Mater. Sci. Eng. A* **2006**, *420*, 1–7. [CrossRef]
10. Eskin, D.; Zuidema, J.; Savran, V.; Katgerman, L. Structure formation and macrosegregation under different process conditions during DC casting. *Mater. Sci. Eng. A* **2004**, *384*, 232–244. [CrossRef]
11. Jones, S.; Rao, A.K.P.; Fan, Z. Melt conditioned direct chill (MC-DC) casting of Al alloys. *Trans. Indian Inst. Met.* **2013**, *66*, 117–121. [CrossRef]
12. Aliravci, C.A.; Gruzleski, J.E.; Pekgüleryüz, M.Ö. A Thermodynamic Study of Metastable Al-Fe Phase Formation in Direct Chill (DC)-Cast Aluminum Alloy Ingots. In *Essential Readings in Light Metals: Volume 3 Cast Shop for Aluminum Production*; Springer: Cham, Switzerland, 2016; pp. 466–474.
13. Zhao, J.; Guo, Y.; Xu, B.; Gu, C.; Wang, Y.; Tang, Q. Effect of Microstructure Evolution of Iron-Rich Intermetallic Compounds on Mechanical Property of Al–7Si–0.3 Mg Casting Alloy with Low Iron Content. *Metall. Trans. B* **2022**, *53*, 1–13. [CrossRef]
14. Sweet, L.; Taylor, J.A.; Couper, M.J.; Easton, M.A. Hot tearing in Al-Mg-Si alloys with minor additions of Cu or Mn. *Mater. Sci. Forum* **2011**, *693*, 217–223. [CrossRef]
15. Ludwig, O.; Drezet, J.-M.; Martin, C.L.; Suéry, M. Rheological behavior of Al-Cu alloys during solidification constitutive modeling, experimental identification, and numerical study. *Metall. Trans. A* **2005**, *36*, 1525–1535. [CrossRef]
16. Feng, Y.; Založnik, M.; Thomas, B.G.; Phillion, A.B. Meso-scale simulation of liquid feeding in an equiaxed dendritic mushy zone. *Acta Mater.* **2020**, *9*, 100612. [CrossRef]
17. Sha, G.; O'reilly, K.; Cantor, B.; Worth, J.; Hamerton, R. Growth related metastable phase selection in a 6xxx series wrought Al alloy. *Mater. Sci. Eng. A* **2001**, *304–306*, 612–616. [CrossRef]
18. Warrington, D.; Mccartney, D.G. Hot-cracking in Aluminium Alloys 7050 and 7010—A Comparative Study. *Cast Met.* **1990**, *3*, 202–208. [CrossRef]

19. Jorstad, J.; Pan, Q.; Apelian, D. Solidification microstructure affecting ductility in semi-solid-cast products. *Mater. Sci. Eng. A* **2005**, *413–414*, 186–191. [CrossRef]
20. Radetić, T.; Popović, M.; Alil, A.; Markoli, B.; Naglič, I.; Romhanji, E. Effect of homogenization temperature on microstruct ure and mechanical properties of Al-Mg-Si alloy containing low-melting point elements. *J. Alloys Compd.* **2022**, *902*, 163719. [CrossRef]
21. Mbuya, T.O.; Odera, B.O.; Ng'ang'a, S.P. Influence of iron on castability and properties of aluminium silicon alloys: Literature review. *Int. J. Cast Met. Res.* **2003**, *16*, 451–465. [CrossRef]
22. Sweet, L.; Easton, M.A.; Taylor, J.A.; Grandfield, J.F.; Davidson, C.J.; Lu, L.; Couper, M.J.; StJohn, D.H. Hot Tear Susceptibility of Al-Mg-Si-Fe Alloys with Varying Iron Contents. *Metall. Mater. Trans. A* **2012**, *44*, 5396–5407. [CrossRef]
23. Adamiec, J. Assessment of high-temperature brittleness range of the casted alloy AZ91. *Mater. Sci. Forum* **2011**, *690*, 41–44. [CrossRef]